Journal of the European Ceramic Society **15** (1995) 319–328

0955-2219/95/$9.50

The Oxidation Behaviour of a Porous Si_2N_2O–ZrO_2 Composite Material

Colette O'Meara,[a] Maiken Heim[b] & Robert Pompe[c]

[a] Department of Physics and [b]Department of Inorganic Chemistry, Chalmers University of Technology and University of Göteborg, S-412 96 Göteborg, Sweden
[c] Swedish Ceramic Institute, Box 5403, S-402 29 Göteborg, Sweden

(Received 13 May 1994; accepted 20 June 1994)

Abstract

The oxidation behaviour of a low-cost, porous Si_2N_2O–ZrO_2 composite material produced without the use of sintering aid was investigated in air between 1000 and 1520°C. The extent of internal oxidation was found to be dependant on the oxidation temperature. At temperatures ≤ 1300°C considerable internal oxidation of the material occurs with concommitant large weight gains. The material exhibits excellent oxidation resistance at high temperatures (>1300°C) and the higher the oxidation temperature the lower the weight gain. A very thin layer of oxide primarily consisting of $ZrSiO_4$ forms on the internal pore walls which, together with the surface oxide layer, protects the material from further oxidation. At 1300°C the stresses induced in the matrix by the volume expansion of the oxidation products cause severe cracking of the material on cooling from the annealing temperature. Following oxidation exposures at temperatures ≥1300°C the unstabilised ZrO_2 phase in the matrix is inhibited from undergoing the t–m *transformation. This is most probably due to the dissolution of nitrogen in ZrO_2 resulting in the stabilised, non-transformable* t'-ZrO_2 *phase.*

1 Introduction

The improvement in toughness hoped for by the inclusion of partially stabilised zirconia into a silicon nitride-based matrix has not been realised. This is mainly due to the additional stabilisation of zirconia by nitrogen which prevents the martensitic transformation from *t–m* ZrO_2 under mechanical stress.[1] In addition, the formation of oxidation prone zirconia oxynitride phases during material fabrication inhibits the use of these materials at intermediate temperatures (500–800°C) and the results from high-temperature oxidation studies are not promising.[2,3]

In this work a Si_2N_2O–ZrO_2 composite is examined which has been produced for high-temperature application. The material has been fabricated by the NPS technique without the use of sintering aid/stabiliser. Nitridation and subsequent reaction sintering via the reaction: $Si_3N_4 + ZrSiO_4 \rightarrow 2\ Si_2N_2O + ZrO_2$ results in a porous microstructure consisting of Si_2N_2O and unstabilised ZrO_2 and which avoids the formation of undesirable zirconium oxynitride phases. The high-temperature behaviour of porous silicon-based materials differs considerably from that of dense materials because of the inherent open porosity. Although the oxidation rate will be correlated to the net area available for reaction it has been found that the rate of oxidation appears to decrease at higher temperatures. This paper examines the oxidation behaviour of the porous composite in the temperature range 1000–1520°C.

2 Experimental

2.1 Material

A Si_2N_2O–ZrO_2 composite, fabricated without sintering aid by the NPS technique from Si and $ZrSiO_4$ was used in this work. The material was produced at the Swedish Ceramic Institute.[4,5] The as-received density was determined to be 2·55 g/cm^3 or 72·4% of TD with 24·5% open porosity. The stoichiometric composition of the sintered material was 64 wt% Si_2N_2O and 36 wt% ZrO_2.

2.2 Oxidation exposures

Specimens for oxidation were cut with a diamond saw into samples of dimensions 3 × 4 × 10 mm, polished with various grades of SiC paper and then ultrasonically cleaned in acetone and alcohol. Sample holders of Al_2O_3 were used. The samples were oxidized in an alumina tube furnace in the range 1000–1520°C in flowing dry air with 6 l/h

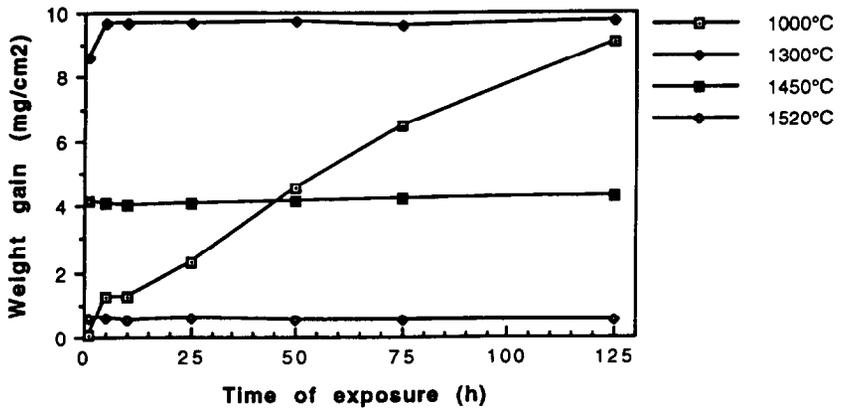

Fig. 1. Weight gain of Si_2N_2O–ZrO_2 material exposed at various oxidation temperatures.

flow rate. The samples were intermittently taken out from the furnace and weighed on an analytical balance with ±5 μg sensitivity. In so doing all the samples were rapidly cooled/reheated to the oxidation temperature. This procedure thus also reflected the effect of cycling on the stability of the oxide scale. Other samples were subjected to the same procedure for up to 250 h but when removed from the furnace were used for SEM examination and pore characteristic determinations. Additional oxidation experiments were carried out at 1450°C to examine the effect of scale removal on the weight gain. The samples were oxidized for 1 h, removed from the furnace and weighed. The oxide scale was then taken away by grinding. The samples were then exposed for another hour at the same temperature.

2.3 Microstructural analysis

Phase analysis of the as-sintered and oxidized materials was carried out by X-ray diffractometry (XRD) using a SIEMENS X-ray diffractometer (D5000). Slices of the material of dimensions *ca* 1 cm^2 were exposed in a thermobalance for 7 h at temperatures between 1000 and 1600°C. The X-ray penetration depth was calculated to be 56 μm at $2\Theta = 65°$. The microstructure of as-sintered material was characterised by analytical transmission electron microscopy (TEM/STEM/EDX) in a Jeol 2000 FX TEM/STEM instrument. The microstructure of the oxidised materials was investigated by analytical scanning electron microscopy in surface and cross-section using a CAM Scan S-4 80DV scanning electron microscope (SEM) equipped with a Link eXL EDX analysis system.

2.4 Determination of pore characteristics

All investigations have been carried out on whole unpowdered samples.

2.4.1 Determination of the surface area by nitrogen adsorption

The BET method was used to determine the internal surface area of the material. Specimens of unexposed and oxidized material were degased at 250°C in a Desorb 2300A for 100 min. The measurements were made in a Flowsorb II 2300 (Micromeritics) using N_2 as adsorbant. Around a 10% mean deviation can be expected at low surface areas (1–2 mg^2/g).

2.4.2 Determination of the density by water penetration

The bulk density was determined using Archimedes' principle. The dry weight was first measured,

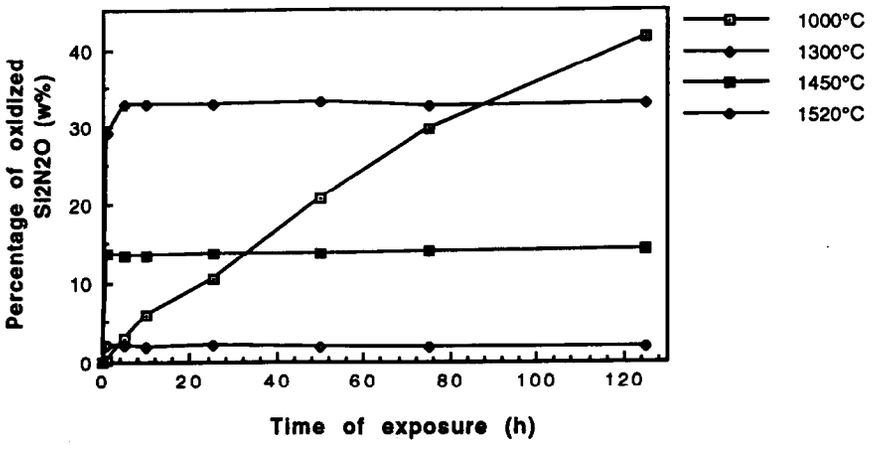

Fig. 2. The percentage of oxidized Si_2N_2O in Si_2N_2O–ZrO_2 material exposed at various oxidation temperatures.

the samples were put under vacuum (<25 mm Hg) for 30 min, then covered with distilled water (under vacuum) and left to soak for 12 h. The wet weight in air and in water was measured and the bulk density was calculated.

2.4.3 Determination of the porosity by mercury porosimetry

The open porosity and volume distribution of the porosity have been measured with the aid of mercury porosimetry using a Micromeritics Poresizer 9305 instrument. The registration of the pressure and the mercury volume intruded in the sample are related to the volume distribution of the pores.

3 Results

3.1 Weight gain versus time curves

The measured oxidation isotherms for samples cyclically oxidized at 1000, 1300, 1450 and 1520°C are shown in Fig. 1. A linear weight increase is observed for material oxidised at 1000°C. The rate of weight gain does not decrease even after long exposure times. At temperatures >1000°C the initial weight gain decreases with increasing oxidation temperature being lowest at 1520°C. At these high temperatures the isotherms show that the maximum weight gain occurs in the first 5 h of exposure after which little or no weight gain takes place.

The oxidation mass balance reaction for the composite is:

$$Si_2N_2O\text{–}ZrO_2 + 3/2O_2 \rightarrow ZrSiO_4 + SiO_2 + N_2(g) \quad (1)$$

As can be seen from eqn (1) ZrO_2 does not contribute to the mass change. Based on the weight change obtained for each measurement at a given temperature, the percentage of reacted Si_2N_2O was calculated and is shown in Fig. 2. In the case of complete oxidation the total weight gain was calculated to be 12·38 wt%. As can be seen from Fig. 1 this percentage was not reached experimentally.

Fig. 3. TEM micrograph showing the general microstructure of as-received Si_2N_2O–ZrO_2 material to consist of sub-micron size ZrO_2 grains (Z) homogeneously distributed in a matrix of sub-micron size Si_2N_2O crystals.

Table 1. Surface phase composition at different oxidation temperatures for Si_2N_2O–ZrO_2 material

Temperature (°C)	*Exposure time (h)*	*Phase composition*				
		Si_2N_2O	*m–ZrO_2*	*t(t')-ZrO_2*	*$ZrSiO_4$*	*SiO_2*
As-received	7	s	s	w	—	—
1000	7	s	s	w	w	w
1300	7	w	w	m	m	w
1450	7	w	w	m	m	w
1600	7	w	w	m	vs	w

w—weak, m—medium, s—strong, vs—very strong.

For the reoxidation experiments at 1450°C the weight increase after reoxidation was found to be approximately 10% of the original weight increase.

3.2 Microstructural analysis

3.2.1 XRD

The identification of oxidation products and phase changes at the various oxidation temperatures and times is detailed in Table 1.

XRD of the surface of the oxidized materials shows an increasing volume of oxidation products, $ZrSiO_4$ and SiO_2, to be present in the scales with increasing temperature reflecting an increasing surface scale thickness. Little amorphous material could be detected. The proportion of *t*–ZrO_2 in the matrix is seen to increase following oxidation at temperatures ≥1300 with a concommitant decrease in the amount of *m*–ZrO_2 as compared with the as-sintered material.

3.2.2 TEM

As shown in Fig. 3 the general microstructure of the as-received material consists of a matrix of sub-micron Si_2N_2O grains in which sub-micron size ZrO_2 grains are homogeneously distributed. The plate-like Si_2N_2O crystals are randomly oriented and of high aspect ratio. The zirconia grains are observed to have an irregular intergranular morphology and were identified by electron diffraction to be predominantly monoclinic (Fig. 4). Small volumes of an amorphous phase surround the matrix grains. Regions of incomplete sintering, containing small (≤ 50 nm) Si_2N_2O grains in a Si rich amorphous phase were frequently observed. A more detailed description of the microstructure can be found in Ref. 6.

3.2.3 SEM

The specimens were examined in SEM in surface and cross-section using the back-scattered electron mode after 2, 10, 50, 100, 150 and 250 h exposure at each temperature. EDX analysis was carried out on cross-section specimens.

Fig. 4. TEM micrograph showing the monoclinic ZrO_2 phase (m) in as-received Si_2N_2O–ZrO_2 material: (a) bright field and (b) dark field.

(1) 1000°C

Compared with the microstructure of as-received material no unambiguous evidence or indication of external or internal oxidation could be detected in SEM. However on cutting the material for preparation for SEM it was observed visually to have 'whitened' all the way through the matrix indicating extensive internal oxidation.

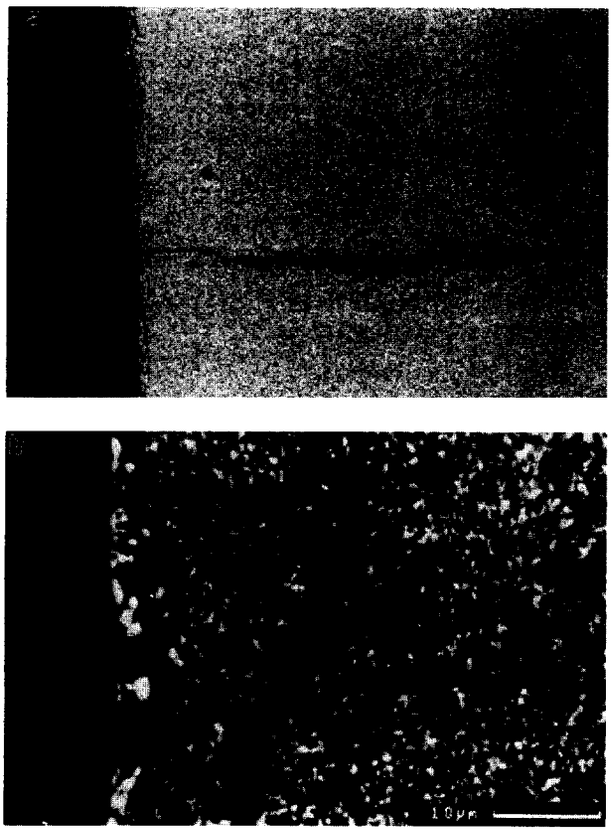

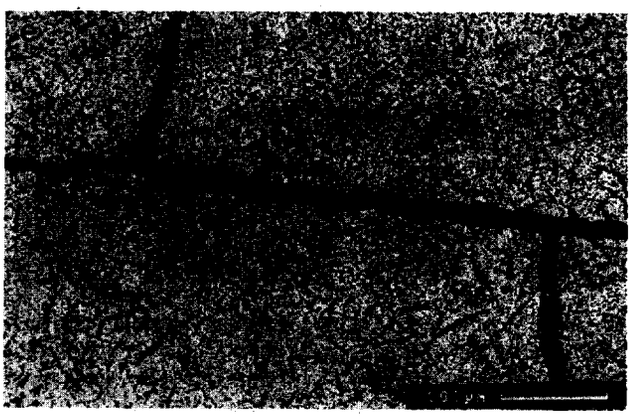

Fig. 5. SEM back-scattered images of the oxide scales of Si_2N_2O–ZrO_2 material exposed at 1300°C. (a) Cross-section showing large cracks in the matrix after 2 h oxidation. (b) Severe cracking observed in the matrix parallel with the surface after 100 h exposure. (c) Cross-section of the oxide scale after 250 h exposure showing $ZrSiO_4$ crystals (Z), crystalline SiO_2 (C) and an amorphous mixed silicate phase (A). (d) A large internal pore in the matrix showing extensive oxidation after 2 h exposure. (e) Oxide surface after 150 h oxidation showing the scale to contain large volumes of $ZrSiO_4$ crystals (Z) and a small volume of crystalline SiO_2 (C).

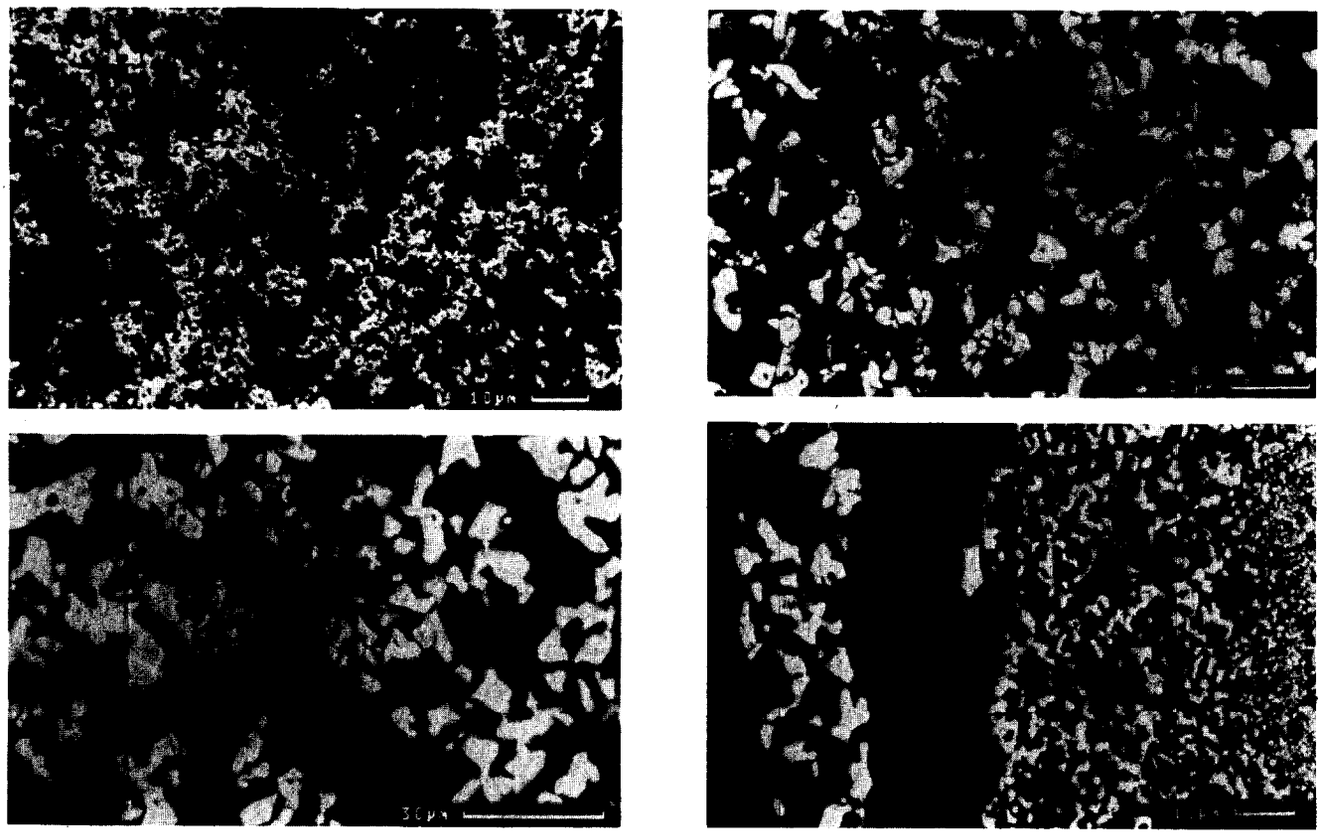

Fig. 6. Back-scattered SEM images of Si_2N_2O–ZrO_2 material exposed at 1450°C. (a) Oxide surface of material exposed for 2 h showing a rough uneven surface. (b) After 100 h extensive cracking of the surface is observed associated with the crystalline silica phase (C). (c) After 250 h the crystalline silica phase (C) assumes a long needle-like morphology. (d) In cross-section duplex scales are seen to form after 50 h exposure showing a region of extensive porosity (P) and a denser outer region with extensive cracking (O).

(2) 1300°C

As is shown in Fig. 5(a) large cracks were observed in the material following oxidation at 1300°C. The cracks frequently extended through the matrix and were of dimensions 10–30 μm in diameter. Additional severe cracking was also observed in the material parallel with and just below the surface (Fig. 5(b)). Cracking associated uniquely with the scale is observed only after longer exposures times (≥100 h). In transverse section thin discontinuous oxide scales ≤2 μm were observed for shorter exposure times. The oxide scale increased in thickness and continuity with time to reach a maximum of approximately 20 μm after 250 h exposure (Fig. 5(c)). Considerable oxidation of larger internal pores was evident in all the specimens (Fig. 5(d)).

As is shown in Fig. 5(e) the scale contained large volumes of small brightly contrasting structures, shown by EDX to contain Zr, Si and O and therefore probably crystalline $ZrSiO_4$, and small volumes of a darker contrasting phase containing Si and O, possibly cristobalite. In addition, an intermediate contrasting phase is observed which contains Si, O and small amounts Fe, Na and K and is possibly an amorphous mixed silicate. The atom number density, size and shape of the crystals increases with increasing exposure time.

(3) 1450°C

Following oxidation at 1450°C the scales have a rough, uneven topography and small cracks are observed within the scale as shown in Fig. 6(a). The cracking of the scale is more extensive after longer oxidation exposures and is observed to be associated with the crystalline silica phase (Fig. 6(b)). A continuous, thick (≤50 μm) oxide scale is observed after short exposure times. No SEM evidence of internal oxidation could be detected.

The phase content of the scales as detected by SEM consists of a large volume of crystalline $ZrSiO_4$, SiO_2 and a mixed silicate phase. After longer oxidation times the atom number density, size and morphology of the crystalline components of the scale show considerable change. The zircon crystals become larger and more particulate with increasing time at temperature as shown in Fig. 6(c). The crystalline silica phase changes in form from almost spheroidal at 100 h to long needle-like grains at 250 h. The scale structure is duplex with an outer more dense region and an inner extensively porous region (Fig. 6(d)).

(4) 1520°C.

After 2 h oxidation at this temperature considerable porosity is observed in the scales in planar section (Fig. 7(a)). With increasing time at temperature the porosity is no longer observed but

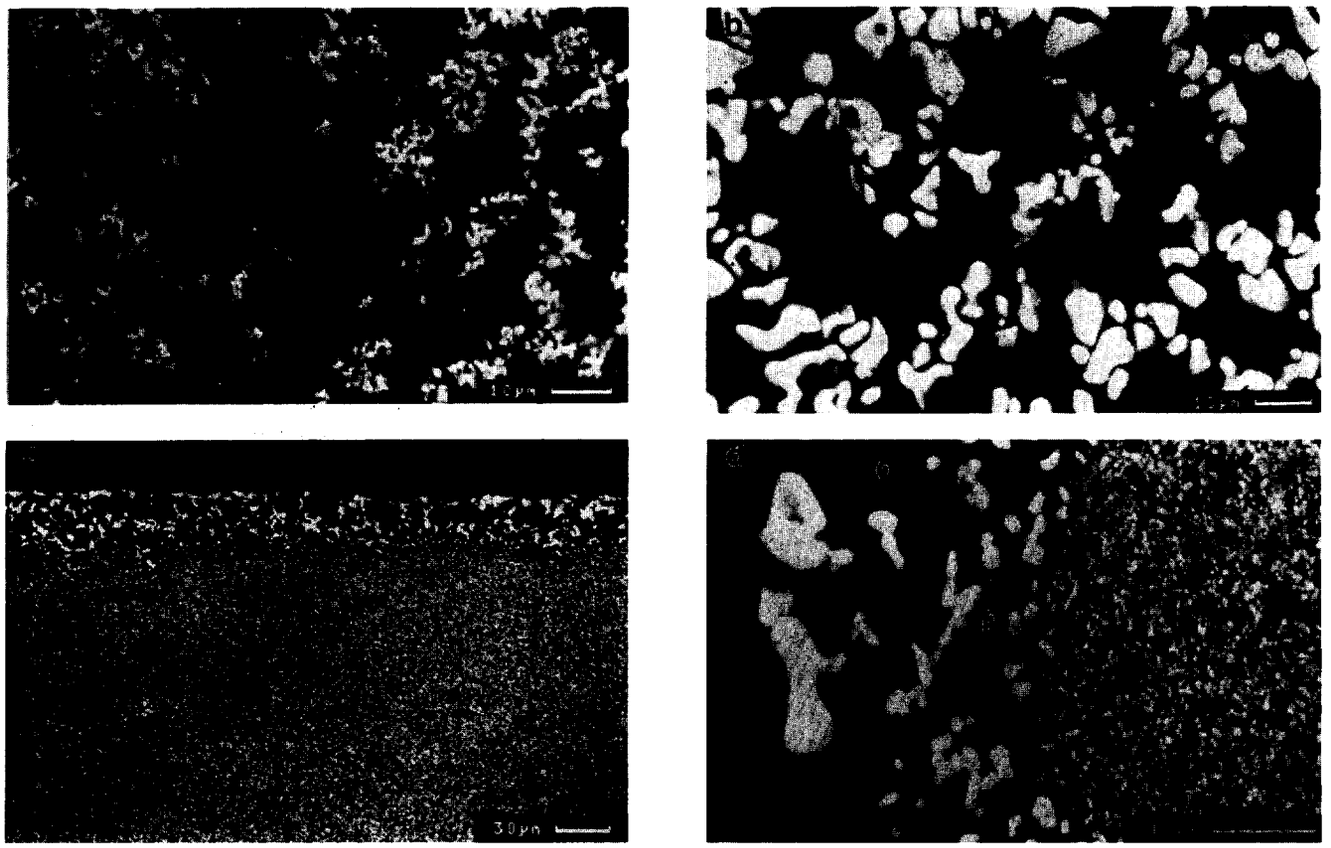

Fig. 7. SEM back-scattered images of Si_2N_2O–ZrO_2 material exposed at 1520°C. (a) Oxide surface after 2 h exposure showing considerable porosity. (b) After 150 h extensive cracking of the surface is observed associated with the crystalline silica phase. (c) Cross-section showing the oxide scale to be up to 50 μm thick after 250 h exposure. (d) Duplex scales are seen to form with a region of extensive porosity (P) and a denser outer region with extensive cracking (O) after 150 h exposure.

extensive cracking is noted associated with the crystalline silica phase (Fig. 7(b)). No evidence of matrix cracking or internal oxidation could be detected. The atom number density of the crystalline components of the scale are observed to increase with increasing time. Duplex oxide scales up to 50 μm thick are seen to develop even at short time exposures at this high temperature. The duplex scale shows extensive porosity in the lower region and extensive cracking in the outer region (Figs 7(c) and (d)).

3.3 Pore characteristics

3.3.1 Specific surface area

The specific surface area of the as-received material was 1·1 ± 0·1 m^2/g. Figure 8 shows selected specific surface area data for samples oxidized for different times at the various oxidation temperatures.

An increase in the specific surface area is observed only at 1000°C. In general the higher the temperature the less the specific surface area differs from that of the as-received material.

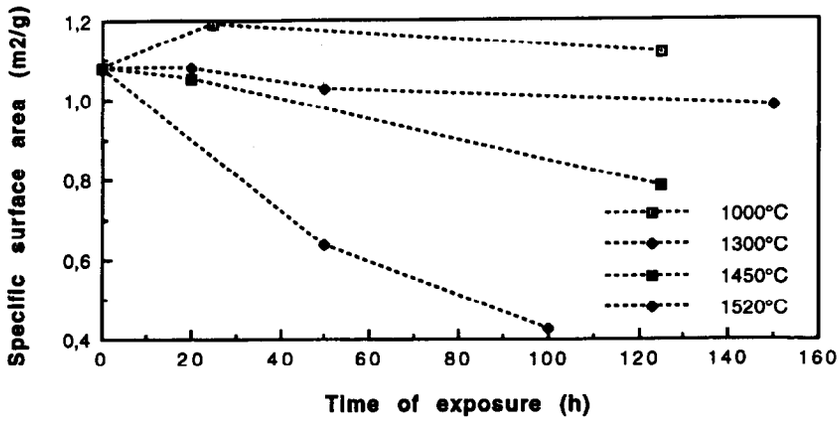

Fig. 8. Specific surface area of Si_2N_2O–ZrO_2 material exposed at various oxidation temperatures.

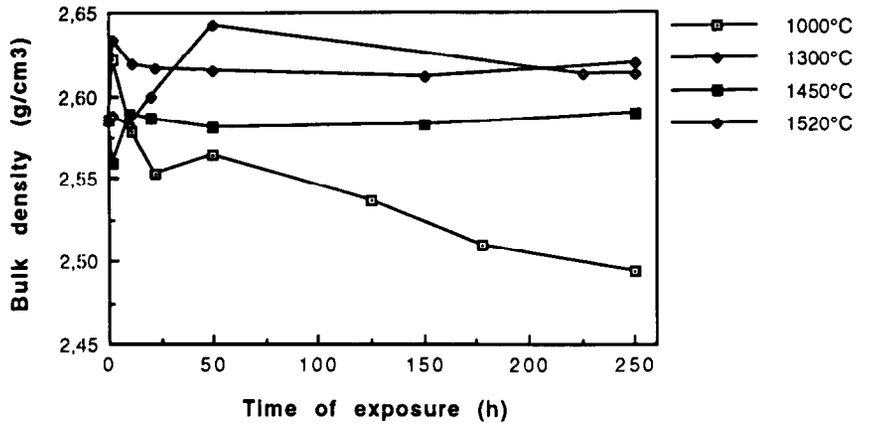

Fig. 9. Bulk density of Si_2N_2O–ZrO_2 material exposed at various oxidation temperatures.

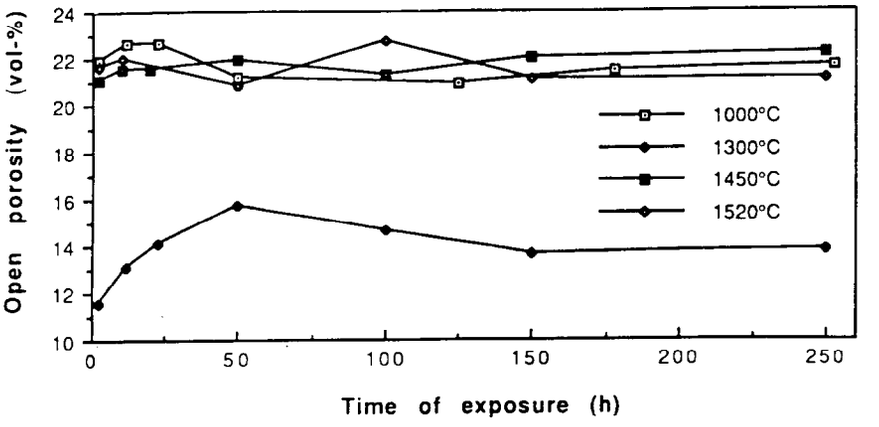

Fig. 10. Open porosity of Si_2N_2O–ZrO_2 material exposed at various oxidation temperatures.

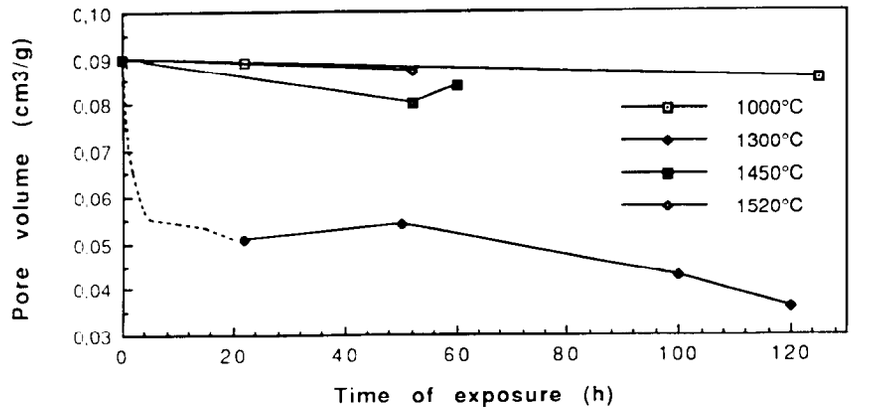

Fig. 11. Pore volume of Si_2N_2O–ZrO_2 material exposed at various oxidation temperatures.

3.3.2 Density

Figure 9 shows the results obtained for the bulk density measurements. The density of the as-received material was determined to be 2·585 g/cm^3.

A significant tendency for density to decrease with time is observed at 1000°C. At all other temperatures the density shows no significant change.

Figure 10 shows the open porosity. The open porosity of as-received material was determined to be 22·3 vol%.

The obtained results show that the open porosity only changes significantly at 1300°C showing a definite decrease.

3.3.3 Pore volume

Porosimetry measurements have been performed on as-received material as well as with oxidized specimens. Figure 11 shows the results for measurements of the pore volume. The pore volume decreases slightly on oxidation at 1000°C. At 1300°C a significant decrease in the pore volume is

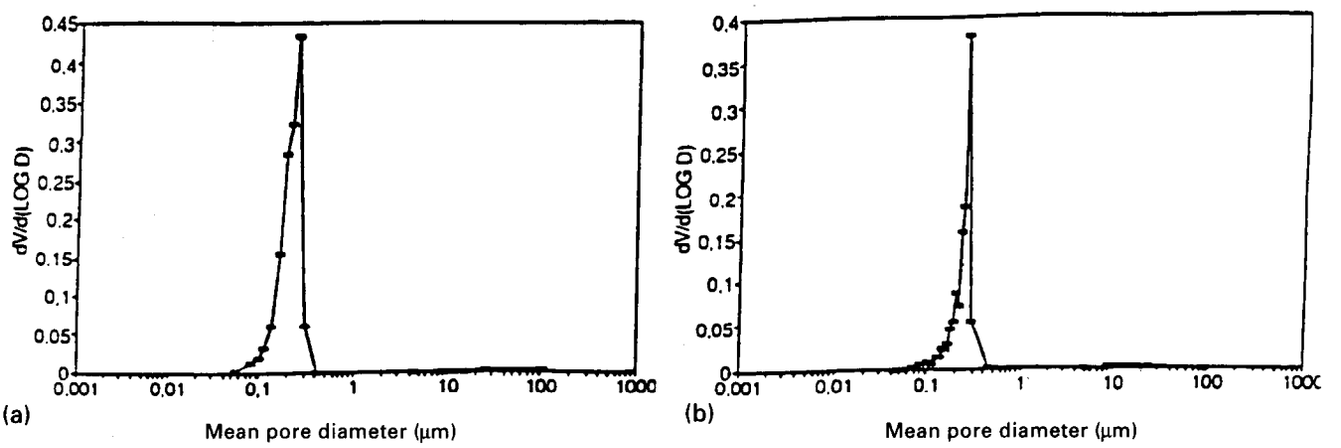

Fig. 12. Pore frequency distribution of a sample of Si_2N_2O–ZrO_2 material: (a) as-received and (b) after oxidation for 120 h at 1300°C.

observed. At higher temperatures the values do not change markedly from that of the as-received material.

Figure 12 shows the pore frequency in as-received material and in a sample exposed for 120 h at 1300°C.

The mean pore diameter is found to be around 0·2 μm. From Fig. 12 it can be seen clearly that neither the mean pore diameter nor the distribution of the pore sizes change significantly.

4 Discussion

In general the results fall into the temperature categories 1000, 1300 and >1300°C in which it is most convenient to discuss the oxidation behaviour.

(1) 1000°C

The linear weight gain curve showing a large and continuous weight increase at this temperature is not consistent with a lack of surface oxide scale formation. The calculations of the percentage of oxidized material show that approximately 40 wt% of the available matrix has reacted. This indicates that a considerable amount of internal oxidation has taken place at this temperature. SEM and XRD show that no oxidation of the ZrO_2 phase had occurred. This implies that oxidation of the Si_2N_2O phase in the pores and pore channels must account for the observed weight gain and results in a thin film of amorphous and crystalline SiO_2 throughout the specimen which could not be detected in SEM. This is reflected in the measured increase in specific surface area, decrease in pore volume and decrease in bulk density as follows:

$$\underset{2\cdot82}{\rho\ (g/cm^3)}\quad Si_2N_2O + 3/2\,O_2 \rightarrow \underset{2\cdot33}{2\,SiO_2} + N_2 \qquad (2)$$

The pores remain open as oxygen diffusion inwards is faster than the oxidation reaction which is slow at this temperature. This results in continued oxidation even after long oxidation times. This type of behaviour is similar to that observed in RBSN materials at low temperatures.

(2) 1300°C

The weight increase is observed to be highest at this temperature and to occur within the first 5 h of exposure. It was calculated that approximately 32 wt% of the Si_2N_2O had been oxidized by this time. This large initial weight increase with formation of thin (2–10 μm) oxide scales is consistent with the occurrence of both internal and external oxidation. As the XRD results show, the ZrO_2 phase is now involved in the oxidation process (eqn (1)) and zircon is formed. This is associated with a large volume increase (~8%). Cristobalite, also detected by XRD and SEM, probably forms during cooling from the oxidation temperature and its formation is also associated with a large increase in volume (~5%). SEM revealed the larger internal pores to be covered with an oxide scale containing zircon, and an Si and O containing phase. Oxidation after the first 5 h is accompanied by a significant decrease in the specific surface area, an increase in density and a decrease in pore volume implying the filling up of internal pores with oxidation products. The oxidation products are of larger volume than the original matrix material and will result in internal stresses and pore filling but will also act as a diffusion barrier to further oxidation. However, due to the volume increase significant internal stresses are built up within the material causing the severe cracking observed at this temperature and which most probably occurred on cooling from the oxidation temperature. If pore closure is responsible for the weight gain stabilisation of the samples after the first 5 h of exposure, then considering the extensive cracking that is observed in the matrix after each cycle, one would expect additional weight gain due to the oxidation of newly exposed surfaces when the samples are replaced in the furnace. However, no additional weight gain is

observed, indicating that complete pore closure does not occur.

The ZrO_2 phase, which is predominantly monoclinic in the as-received material, transforms to t–ZrO_2 at the oxidation temperature (t–m transformation ~1170°C). As it is unstabilised the t-ZrO_2 phase should transform to m-ZrO_2 on cooling. However, the XRD results show t-ZrO_2 to be the main ZrO_2 phase present in the matrix. The inhibition of the t–m transformation can arise from two sources: (i) the stresses in the matrix arising from the volume expansion during internal oxidation mechanically constrain the transformation; and (ii) a high N_2 activity during internal oxidation at these temperatures can result in the dissolution of nitrogen in ZrO_2 forming the stabilised non-transformable t'-ZrO_2 phase. It is possible that both factors contribute to stabilisation but with regard to the similar behaviour observed at higher temperatures (next section) where extensive internal oxidation does not occur, it is thought that nitrogen stabilisation is the most probable explanation and this is presently under investigation in TEM studies.[6]

(3) >1300°C

The material shows excellent oxidation resistance at high temperatures. The weight gain curves show that the higher the oxidation temperature the lower the weight gain. Calculations of the percentage of reacted Si_2N_2O indicate that only 14 and 2 wt% had oxidized at 1450 and 1520°C respectively. This weight gain occurred within the first 2 h of exposure and SEM showed it to be accompanied by the growth of thick predominantly crystalline surface oxide scales (up to 50 μm) with no evidence of internal oxidation. These oxide scales were continuous but considerable microcracking was observed associated with the formation of cristobalite on cooling. Although this implies that rapid external oxidation seals off the surface pores before internal oxidation can occur this does not seem to be the case as the specific surface does not decrease nor is any change noted in pore volume as compared to the as-received material. In addition, in the reoxidation experiments at 1450°C a weight gain of only 10% of the original weight gain (2·7%) was recorded following scale removal and reoxidation. If pore closure was entirely responsible for the low weight gains at this temperature then the weight gain upon reoxidation should be similar to the original weight gain. This indicates that pore closure may not be occurring. Instead, it is thought that the internal pores are rapidly covered with a very thin layer of oxide primarily consisting of $ZrSiO_4$ with small amounts of silica. This layer, together with the surface oxide layer, protects the material from further oxidation which should occur as a result of the surface cracks formed during the thermal cycling excursions.[6]

The XRD results show that the t-ZrO_2 is retained to room temperature as observed following oxidation at 1300°C and is presently under investigation.[6]

In general the oxidation behaviour of the porous composite is similar to that of RBSN material where the oxidation rate is also seen to decrease significantly at higher temperatures. The latter effect has been explained by Davidge who proposed a two stage oxidation process for porous ceramics, namely surface oxidation and the oxidation of the pore channel walls in the interior of the material.[7] At higher temperatures where surface oxidation is more rapid, pore closure will occur before internal oxidation is completed.[9] Although this general trend is similar for the composite as is discussed above, the results of this work indicate that pore closure may not be occurring. Instead it is thought that a very thin layer of oxide primarily consisting of $ZrSiO_4$ forms on the internal pore walls which, together with the surface oxide layer, protects the material from further oxidation. In addition, the composite consists of two highly refractory phases. Although the eutectic of the Si_2N_2O–ZrO_2–SiO_2 system is not known, the XRD results obtained for material exposed at 1600°C show no indications of amorphous material resulting from eutectic melting. This implies that the eutectic temperature lies above 1600°C. The oxidation behaviour is superior to that reported of other Si_3N_4–ZrO_2 or Si_2N_2O–ZrO_2 composites.[2,3,8] The latter have been prepared using metal oxide sintering aids/stabilisers which in general lower the eutectics of the system and decrease the viscosity and softening point of intergranular amorphous phases in the matrix with concommitant decrease in oxidation resistance.

5 Conclusions

(1) In general the trend in the oxidation behaviour of the Si_2N_2O–ZrO_2 composite is similar to that of other porous nitrogen ceramic materials where the oxidation rate is seen to decrease significantly at higher temperatures.

(2) At temperatures ≤1300°C considerable internal oxidation of the material occurs with concommitant large weight gains. At 1300°C the stresses induced in the matrix by the volume expansion of the oxidation products cause severe cracking of the material on cooling from the annealing temperature.

(3) The material exhibits excellent oxidation resistance at high temperatures (>1300°C) and the higher the oxidation temperature the lower the weight gain. Protective oxide scales form at external and internal surfaces within the first 2 h of exposure which inhibit further oxidation. It is thought that narrowing of the pore channels may take place but complete pore closure does not occur.

(4) Following oxidation exposures at temperatures ≥1300°C the unstabilised ZrO_2 phase in the matrix is inhibited from undergoing the *t–m* transformation. This is most probably due to the dissolution of nitrogen in ZrO_2 resulting in the stabilised, non-transformable *t'*-ZrO_2 phase.

Acknowledgements

We would like to thank Dr Vratislav Langer for help with the XRD investigations. Financial support from the Swedish National Board for Industrial and Technical Development (NUTEK) is gratefully acknowledged.

References

1. Cheng, Y., O'Meara, C., Slasor, S., Pompe, R. & Thompson, D. P., Some features and limitations of zirconia toughened nitrogen ceramics. In *Proc. 4th Int. Symp. Ceramic Materials and Components for Engines*, ed. R. Carlsson, T. Johansson & L. Kahlman. Elsevier Applied Science, London, 1992, pp. 657–64.
2. Falk, L. K. L. & Rundgren, K., Microstructure and short-term oxidation of hot-pressed $Si_3N_4/ZrO(+Y_2O_3)$ ceramics. *J. Am. Ceram. Soc.*, **1** (1992) 28–35.
3. O'Meara, C., The microstructure and the oxidation behaviour of Si_2N_2O/ZrO_2 composites. In *Proc. 4th Int. Symp. Ceramic Materials and Components for Engines*, ed. R. Carlsson, T. Johansson & L. Kahlman. Elsevier Applied Science, London, 1992 pp. 252–9.
4. Pompe, R., Method for producing ceramic composite materials containing silicon oxynitride and zirconium oxide. U.S. Pat. No. 438 416, SE. Pat. No. 8702268-7, 1987.
5. Pompe, R., Method for producing ceramic composite materials containing silicon oxynitride and zirconium oxide. Patent Co4B 35/48,35/58,1988.
6. O'Meara, C. & Heim, M. to be presented at ECRS4, Ricione, Italy, October, 1995.
7. Davidge, R. W., Evans, A. G., Gilling, D. & Wilyman, P. R., *Special Ceramics 5*, ed. P. Popper. British Research Association, Manchester, 1972, pp. 329–43.
8. O'Meara, C., Sjöberg, J., Dunlop, G. & Pompe, R., Oxidation of pressureless sintered Si_2N_2O materials. *J. Europ. Ceram. Soc.*, **7** (1991) 369–78.
9. Porz, F. & Thümmler, F., Oxidation mechanism of porous silicon nitride. *J. Mater. Sci.*, **19** (1984) 1283–95.